Bio Synthesis of Zn doped AgTe with the help of Allium Sativum peel powder for bacterial results

Abstract

Telluride is an extremely rare element most commonly used in combination with other metals to increase their machinability and bioactivity due to its mild toxic nature. Bacterial-mediated approaches to tellurium recovery have not been extensively investigated, but have the potential to confer substantial advantages relative to find bacterial activities of Zinc, Silver and its tellurides. Bacteria are currently used to separate a number of elements from their sources, most notably in the bioleaching of Zinc and Silver from their ores. Using biosynthesis method Zn doped AgTe materials were synthesized and characterized by using X-ray Diffractometer, Fourier Transform Spectroscopy and its applications of bacterial results. From structural studies the crystal size was nearly 52 nm, and FTIR spectrometer shows the vibrational frequency of the Zn doped AgTe NPs. Five different bacterial strains both positive and negative and its bioactivity can be measured.

Keywords; Gram negative, Zinc, Silver Telluride and Fourier Transform Spectroscopy

1. Introduction

Nanotechnology industry is expanding at a rapid rate and deep investigation of the health and environmental effects of these materials is necessary. Zn, Ag materials, due to their novel properties, was promising components in a wide range of nanoscale devices for future applications. Zinc and Silver are a versatile semiconductor material with a wide band gap of above 3 to 3.5 eV at room temperature, which has been found useful in many applications such as opto-electronic devices, surface acoustic wave devices, field emitters, piezoelectric devices, transparent conducting materials and solar cells.

Zn, Ag nanoparticles are one of the most promising materials for the fabrication of chemical and biosensors due to having exotic and versatile properties including biocompatibility, nontoxicity, chemical and photochemical stability, high specific surface area, optical transparency, electrochemical activities, high electron communicating features and so on [2] The biosynthesis of Zinc and Silver were achieved by a novel, biodegradable and convenient procedure [3].

Zn doped telluride based semiconductors with wide bandgaps have attracted much interest for blue and blue-green light emitting diodes (LEDs) and Laser diodes (LDs). The poor ohmic contact to P-Zn doped AgTe layers limits the performance of these devices. To minimize the contact problem, highly doped P-type Zn doped AgTe as a contact layer as intermediate semiconducting layers between the metal and P-type Zn doped AgTe have been investigated. Zn doped AgTe alloy is a candidate material for blue-green and yellow LEDs. Zn doped AgTe and related compounds are prepared here by different Bio synthesis method. Spectroscopy has been established as a powerful and useful tool not only in the field of chemistry, but also in physics, biology, medicine, pollution and so on. Every branch of Spectroscopy from microwave to Gamma rays has been effectively used both quantitatively and qualitatively. Advances in IR spectroscopy had a significant impact on analyzing assays for biomedical and biological applications. Both food science and spectroscopic are showing an increasing interest in the medical applications of mid-infrared spectroscopy. The applications of FTIR are being supported as a reliable tool for the analysis of carbohydrate, lipids, fat and protein [4]

2.Experimental

The Allium Sativum, commonly known as garlic, is a species in the onion genus. The peel of this garlic is used as a reducing agent in the synthesis process. Zn doped AgTe NPs

exhibit unique and tunable optical properties on account of their shape and size distribution of the nanoparticles. XRD measurements of the Allium sativum peel mediated synthesized Zn doped with AgTe NPs were carried out. The diffracted intensities were recorded from 30º to 80º angles. The sizes of the nanoparticles were confirmed by using TEM analysis (transmission electron microscopy – Hitachi H-7100 using an accelerating voltage of 120 kV and methanol as solvent).

Fresh peels of Allium sativum were collected, washed thoroughly with double distilled water and dried in air and powdered. About 4 g of Allium Sativum peel powder was mixed with 40 mL of double distilled water at room temperature (25 ^{0}C). This extract was filtered through nylon mesh (Spectrum), followed by Millipore hydrophilic filter (0.22 lm) and used for further experiments [5].

To prepare solution finely powdered samples of ~ 10 gm of AgTe were made with X= 0.6. The starting reagents (Zinc metal basis, 99.9995%; silver telluride, metal basis, 99.999%) were finely ground, mixed in the correct stoichiometry, and sealed in quartz tubes under vacuum. The weighed, 10gm of AgTe with Zn (1.406gm) powder have to taken in the round flask of 100 ml and have to dissolve it in distilled water. Then in an double neck round bottom flask 2 ml of Garlic peel extract and 18 ml of ethanol solvent have to be taken and the prepared this solution of 80 ml have to take in the double neck round bottom flask.

The prepared solution has to be keep for reflexing at 60° C for 1 hr. Then the remaining solution has to be taken under centrifuging. The remaining solution has to taken in centrifuge tubes with an equal quantity. The precipitate like Zn doped AgTe NPs material can be in the centrifuge tubes after centrifuging. The ethanol solution have to poured out and remaining solvent had to keep it in oven under 250° C for 2 hr [6].

Centrifuge: Centrifuges are high-speed rotational instruments to deposit precipitates by the centrifugal force. Centrifuge tubes have a conical bottom that enables to collect a small amount of the sample. Do not use cracked centrifuge tubes, which might be broken upon centrifugation. Keep the sample volume below the half of the tube height, or the liquid might overflow upon centrifugation. Wipe off liquid outside of the tube, or the tube holder might be corroded. Insert a pair of centrifuge tubes in two holders located at opposite positions in a centrifuge. The weights of these tubes containing the samples must be equal [7].

The colors of the solid solutions vary gradually from dark red (AgTe) to brownish yellow (Zn) decreases reflecting the band-gap of the alloy samples smoothly changing in the optical frequency range.

3. Results and Discussion

The homogeneity of the samples was checked using X-ray diffraction by monitoring the width and line-shape of the (241), (212) and (571) Bragg peaks measured on a rotating anode Cu K_{α} source. Finely synthesized powdered samples were sieved through a 200-mesh sieve and then packed into pellets and measured in symmetric reflection geometry. The high intensity (241), (212) and (571) peaks along with other peaks are reproduced in Figure 1. The line-widths are narrow and smoothly interpolate in position between the positions of the end-members (Zn doped AgTe) verifying the homogeneity of the prepared solid solution powder samples. The prepared material has orthorhombic structure having lattice constants as according to JCPDS file No, 8.90Aº, 20.07Aº and 4.62Aº this value is well matched with the results of 8.15 Aº, 20.96 Aº and 4.67 Aº. The crystal size was measured as 52 nm [8].

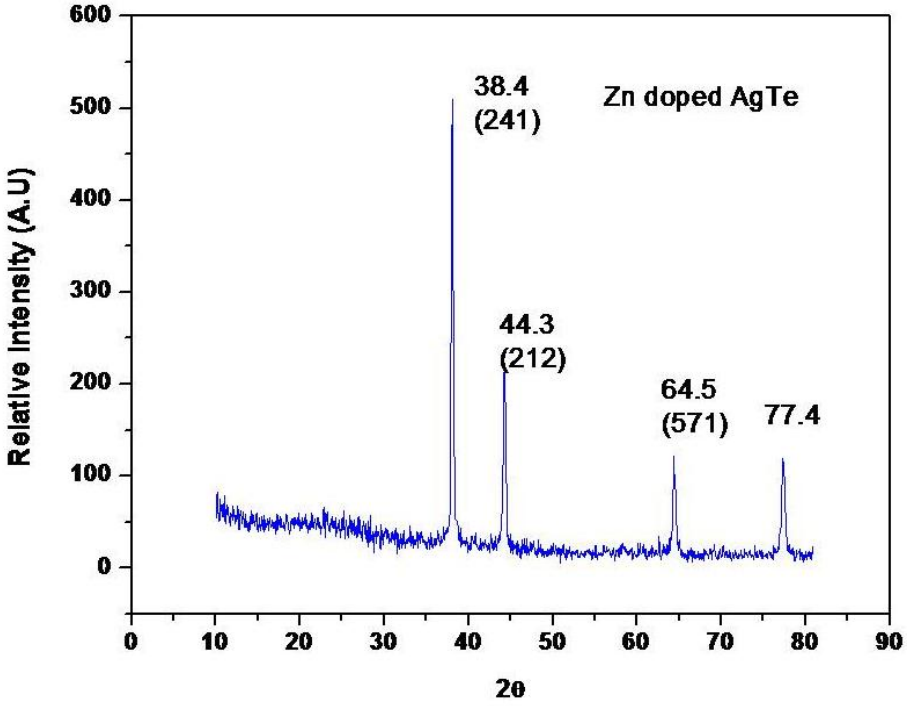

Figure 1 XRD Analysis of Zn doped AgTe Nanoparticles

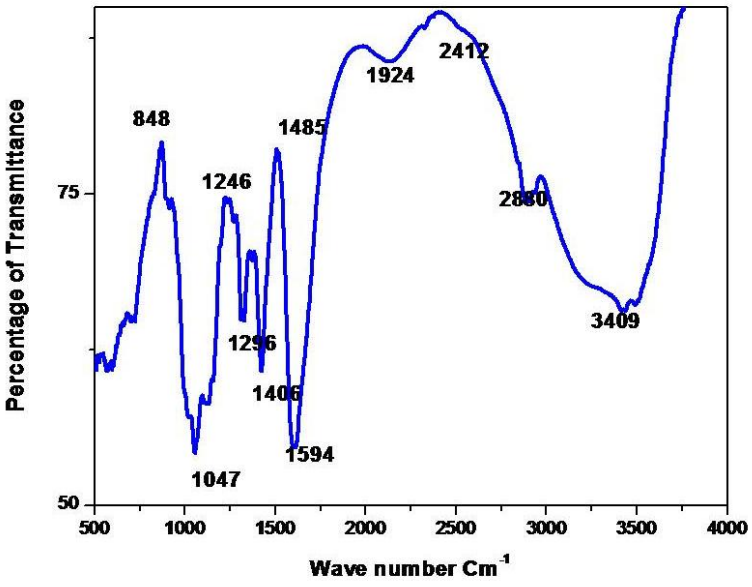

Figure 2 FTIR Analysis of Zn doped AgTe Nanoparticles

According to Zn produces the effect it serves as the production layer for high reactive AgTe materials. It improves the optical performance and bioactivity. A similar result was reported in Zn interstial atoms of NPs [9].

Figure 2 shows FTIR spectrum of Zn doped AgTe NPs, prepared for the sharp and intense peak at 848 cm^{-1} is attributed OH antisymmetric stretching vibrations in the crystal structure of Zn doped AgTe NPs. The peak at around 1406 cm^{-1} is assigned to the Zn-Ag stretching vibration in Ag-Te [10]. The 1406 cm^{-1} ,1594 corresponds to the bending vibration of OH-C-O, stretching vibrations respectively. The other peaks at 2880$cm^{-1}$and 1924$cm^{-1}$are due to the stretching and the bending vibration of water respectively. The broad peaks of Zn doped AgTe NPs 3409 $cm^{-1}$and 2880$cm^{-1}$is due to the stretching and bending vibration of water respectively. 1924 cm^{-1} is the bending vibration of OH bond. Absence of 3409cm^{-1} sharp peak due to antisymmetric stretching vibration in the Zn doped AgTe biosynthesized NPs. The overall observation from the recorded spectra shows well defined and intense absorption from the recorded spectra shows well defined and intense absorption over the wavelength under study. Generally this indicates that the vibrations of the functional groups corresponding to the wavelength of absorptions are well defined within the chemical environment [11].

The TEM image of the synthesized sample is shown in Figure 3a, from the Figure 3b it is seen SAED pattern, that spherical shaped Zn doped AgTe NPs along with some needle shaped particles are produced. Due to the collective coherent excitation of the pre electron in conduction band in a metal NPs, strong agglomeration of the particle produces scattering of light by the particles takes place. It exhibited flakes like structure formed due the aggregation of NPs. It can be seen that the concentration of Zn significantly affects the shape of Zn doped AgTe NPs. With increasing the agglomeration the sizes of the NPs increases, thereby increasing the density

of NPs. In addition the structures are interconnected with the adjacent bonds of Zn with AgTe NPs, such that no clear boundary exists between one another [12].

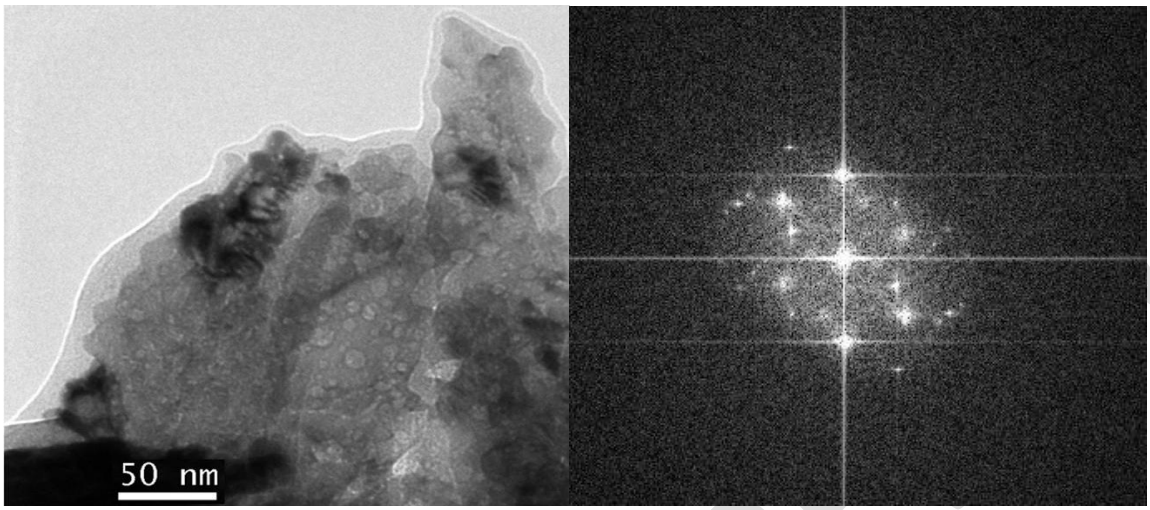

Figure 3(a-b) TEM with SAED Pattern Analysis of Zn doped AgTe Materials

Antibacterial activity of Zn doped AgTe Nanomaterials

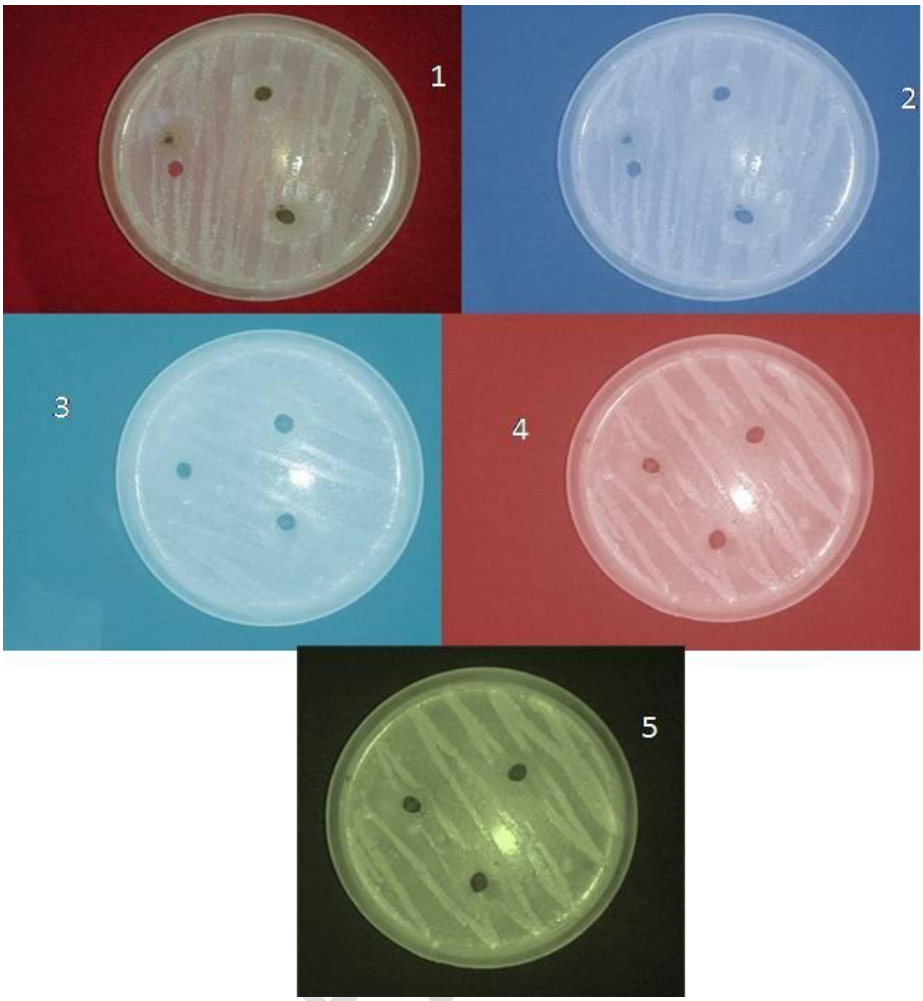

Figure 4. Anti bacterial studies of Zn doped AgTe NPs

Table-1 Antibacterial activity of Zn doped AgTe Nanomaterials

S. No	Bacteria	Zone of Inhibition (mm)		
		5mg	10mg	25mg
1.	Escherichia coli	5	10	11
2.	Pseudomonas aeruginosa	13	17	18
3.	Proteus mirabilis	12	15	17
4.	Streptococcus mutans	12	13	18
5.	Bacillussubtilis	9	10	14

In this particular case, antibacterial capability of a Zn doped AgTe synthesized material depends on the following factors (i) population of reactive oxygen species (ROS), (ii) Number of Ag^{2+} Zn^{2+} and Te^{2+}ions released and(iii) Structure and its size of the particles. To counterparts in all these factors the surface active catatonics Ag^{2+}, Zn^{2+} and Te^{2+} NPs synthesized in the current research are investigated against the bacterial organisms such as Escherichia coli (*Gram-negative*),Pseudomonas aeruginosa (*Gram-negative*), Proteus mirabilis (*Gram-negative*), Streptococcus mutans (*Gram-positive*) and Bacillus subtilis ((*Gram-positive*) [13]. After the thorough and careful examination on the XRD, FTIR and TEM with EDAX analysis it is found to exhibition more number of double cationic series so called Reactive Oxygen Species (ROS) are inhibited the bacterium in an extraordinary manner nearly within 5 hours.].

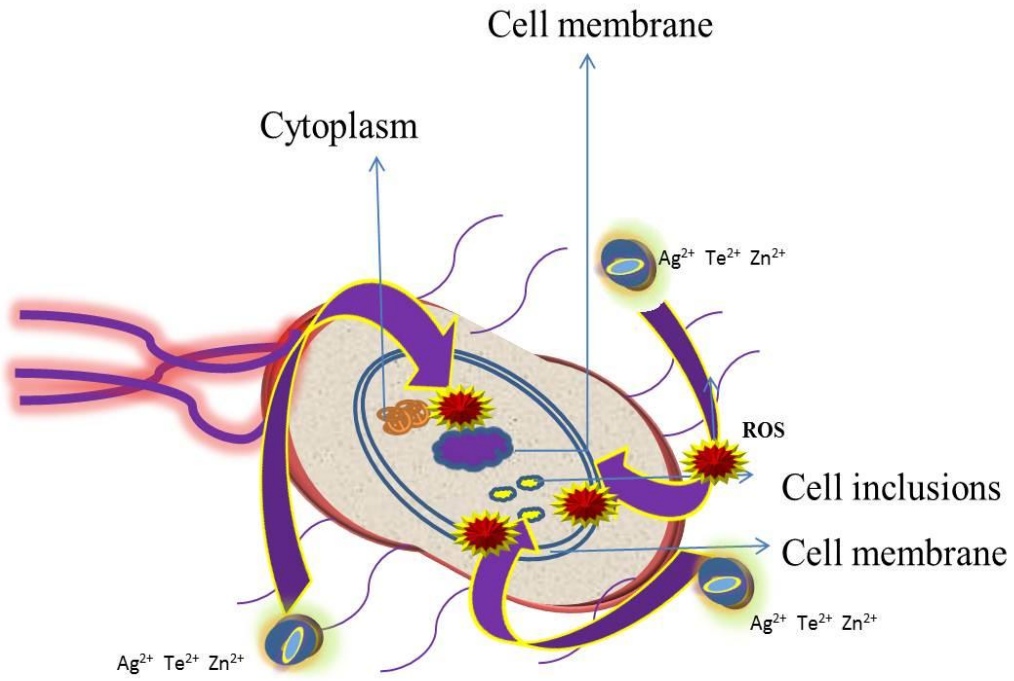

Figure 5. Described mechanism for the enhanced antibacterial activity of double cationic Ag^{2+}, Zn^{2+} and Te^{2+}

Due to the electromagnetic interaction between the bacterial cell and these cations, the nanoparticles enter through the cell walls and penetrating and damaging the cell system of bacterium. The generation of ROS further makes the damage and cell became deformed. Moreover Zinc inertials (Zn), Telluride interstitials (Te) and silver interstitials (Ag) in this system are also contributed to damage all the bacterial cell systems [14]. The possible mechanism for the enhanced antibacterial efficiency of the double cationic doped system is clearly epitomized in Figure 5.This mechanism is strongly supported by the series of double cationics nanoparticles formed in the case of doping. Thereby antimicrobial ions are liberated and give the ZOI due to the inertial and number of ROS formation effectively [15].

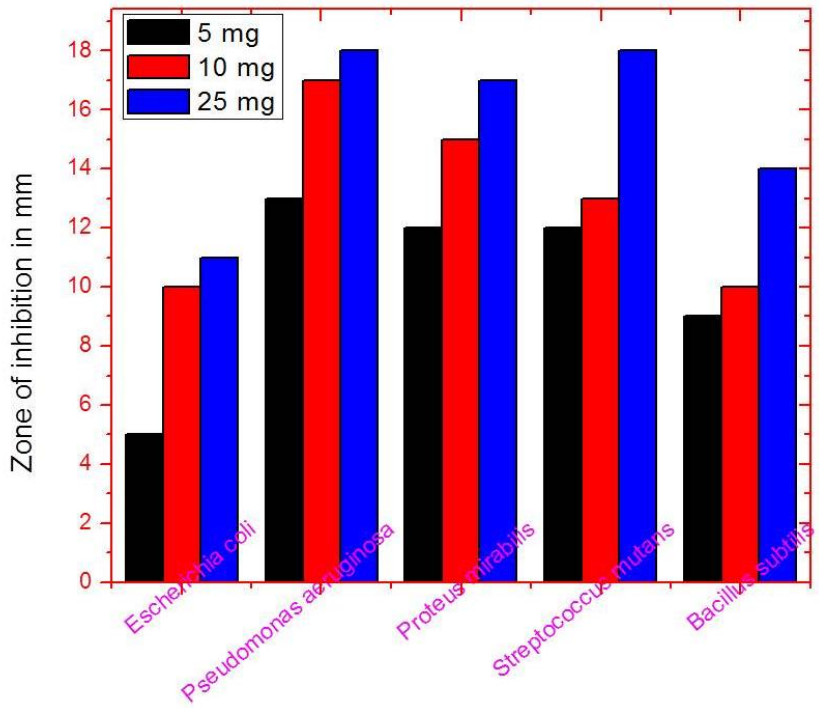

Figure 6. Zone of inhibition produced by Zn doped AgTe NPs against (a) Escherichia coli (b) Pseudomonas aeruginosa, (c) Proteus mirabilis, (d) Streptococcus mutans, (e) Bacillus subtilis

4. Conclusion

Irrespective of whether bacterial transformation of tellurite is a detoxification strategy or an 'unintended' by-product of cellular reducing agents, to understand the complex interactions, including the enzymatic reactions, between bacteria and tellurium of Zn doped AgTe materials. The structural studies infer the crystal size of 52 nm. Results revealed potential activity against, Gram positive, Gram negative and multidrug resistant strains and it was selected and identified based on their biochemical, morphological characteristics. Present study indicated that more than 50% of the bacterial strains revealed promising antibacterial activity against the tested Gram positive and negative bacteria.

References

[1]. Bassora, B.K., Da Costa, C.E., Gariani, R.A., Comasseto, J.V. and Dos Santos, A.A., 2007. Tellurium in organic synthesis: synthesis of bioactive butenolides. *Tetrahedron letters*, *48*(8), pp.1485-1487.

[2].Wendler, E.P. and Dos Santos, A.A., 2009. The use of butyl organotellurides in the synthesis of natural bioactive compounds. *Synlett*, *2009*(07), pp.1034-1040.

[3].Melliou, E. and Chinou, I., 2005. Chemistry and bioactivity of royal jelly from Greece. *Journal of agricultural and food chemistry*, *53*(23), pp.8987-8992.

[4].Gomez-Vega, J.M., Saiz, E., Tomsia, A.P., Oku, T., Suganuma, K., Marshall, G.W. and Marshall, S.J., 2000. Novel bioactive functionally graded coatings on Ti6Al4V. *Advanced Materials*, *12*(12), pp.894-898.

[5].Briand, E., Gu, C., Boujday, S., Salmain, M., Herry, J.M. and Pradier, C.M., 2007. Functionalisation of gold surfaces with thiolate SAMs: Topography/bioactivity relationship–A combined FT-RAIRS, AFM and QCM investigation. *Surface Science*, *601*(18), pp.3850-3855.

[6].Liu, C.L., Wu, H.T., Hsiao, Y.H., Lai, C.W., Shih, C.W., Peng, Y.K., Tang, K.C., Chang, H.W., Chien, Y.C., Hsiao, J.K. and Cheng, J.T., 2011. Insulin-directed synthesis of fluorescent gold nanoclusters: preservation of insulin bioactivity and versatility in cell imaging. *Angewandte Chemie International Edition*, *50*(31), pp.7056-7060.

[7].Zhang, L., Yu, J.C., Mo, M., Wu, L., Kwong, K.W. and Li, Q., 2005. A General in situ Hydrothermal Rolling-Up Formation of One-Dimensional, Single-Crystalline Lead Telluride Nanostructures. *Small*, *1*(3), pp.349-354.

[8].Toman, R., Garidel, P., Andrä, J., Slaba, K., Hussein, A., Koch, M.H. and Brandenburg, K., 2004. Physicochemical characterization of the endotoxins from Coxiella burnetii strain Priscilla in relation to their bioactivities. *BMC biochemistry*, *5*(1), p.1.

[9].Yang, S., Jia, W.Z., Qian, Q.Y., Zhou, Y.G. and Xia, X.H., 2009. Simple approach for efficient encapsulation of enzyme in silica matrix with retained bioactivity. *Analytical chemistry*, *81*(9), pp.3478-3484.

[10].Rosellini, E., Barbani, N., Giusti, P., Ciardelli, G. and Cristallini, C., 2010. Novel bioactive scaffolds with fibronectin recognition nanosites based on molecular imprinting technology. *Journal of applied polymer science*, *118*(6), pp.3236-3244.

[11].Achilonu, M.C. and Umesiobi, D.O., 2015. Bioactive phytochemicals: bioactivity, sources, preparations, and/or modifications via silver tetrafluoroborate mediation. *Journal of Chemistry*, *2015*.

[12]. Saleem, A.M., Prabhavathi, G., Karunanithy, M., Ayeshamariam, A. and Jayachandran, M., 2018. Green Synthesis of Nanoparticle by Plant Extracts—A New Aproach in Nanoscience. *Journal of Bionanoscience*, *12*(3), pp.401-407.

[13].Rasool, K. and Lee, D.S., 2016. Effect of ZnO nanoparticles on biodegradation and biotransformation of co-substrate and sulphonated azo dye in anaerobic biological sulfate reduction processes. *International Biodeterioration & Biodegrada*, *109*, pp.150-156.

[14].Feris, K., Otto, C., Tinker, J., Wingett, D., Punnoose, A., Thurber, A., Kongara, M., Sabetian, M., Quinn, B., Hanna, C. and Pink, D., 2009. Electrostatic interactions affect nanoparticle-mediated toxicity to gram-negative bacterium Pseudomonas aeruginosa PAO1. *Langmuir*, *26*(6), pp.4429-4436.

[15]. El-Damrawi, G., Doweidar, H. and Kamal, H., 2017. Characterization of new categories of bioactive based tellurite and silicate glasses. *Silicon*, *9*(4), pp.503-509.